Sedimentology (2005) **52,** 271–289 doi: 10.1111/j.1365-3091.2004.00694.x

Mass movement-induced fold-and-thrust belt structures in unconsolidated sediments in Lake Lucerne (Switzerland)

MICHAEL SCHNELLMANN*, FLAVIO S. ANSELMETTI*, DOMENICO GIARDINI† and JUDITH A. McKENZIE*
**Geological Institute, Swiss Federal Institute of Technology, ETH Zentrum, CH-8092 Zürich, Switzerland (E-mail: michael.schnellmann@alumni.ethz.ch)*
†Institute of Geophysics, Swiss Federal Institute of Technology, ETH Hönggerberg, CH-8093 Zürich, Switzerland

ABSTRACT

High-resolution seismic imaging and piston coring in Lake Lucerne, Switzerland, have revealed surprising deformation structures in flat-lying, unconsolidated sediment at the foot of subaqueous slopes. These deformation structures appear beneath wedges of massflow deposits and resemble fold-and-thrust belts with basal décollement surfaces. The deformation is interpreted as the result of gravity spreading induced by loading of the slope-adjacent lake floor during massflow deposition. This study investigated four earthquake-triggered lateral mass-movement deposits in Lake Lucerne affecting four sections of the lake floor with areas ranging from 0·25 to 6·5 km^2 in area. Up to 6 m thick sediment packages draping the subaqueous slopes slid along the acoustic basement. The resulting failure scars typically lie in water depths of >30 m on slopes characterized by downward steepening and inclinations of >10°. From the base-of-slope to several hundred metres out onto the flat plains, the wedges of massflow deposits overlie deeply (10–20 m) deformed basin-plain sediment characterized by soft sediment fold-and-thrust belts with arcuate strikes and pronounced frontal thrusts. The intensity of deformation decreases towards the more external parts of the massflow wedges. Beyond the frontal thrust, the overridden lake floor remains mostly undisturbed. Geometrical relationships between massflow deposits and the deformed basin-plain sediment indicate that deformation occurred mainly during massflow deposition. Gravity spreading induced by the successive collapse of the growing slope-adjacent massflow wedge is proposed as the driving mechanism for the deformation. The geometry of fjord-type lakes with sharp lower slope breaks favours the deposition of thick, basin-marginal massflow wedges, that effectively load and deform the underlying sediment. In the centre of the basins, the two largest massflow deposits described are directly overlain by thick contained (mega-)turbidites, interpreted as combined products of the suspension clouds set up by subaqueous mass movements and related tsunami and seiche waves.

Keywords Fold-and-thrust belt, gravity spreading, high-resolution seismic data, lacustrine sedimentation, massflow, translational slide.

INTRODUCTION

Mass movements are common features in marine and lacustrine systems. They represent significant sediment accumulation processes and can be a considerable hazard in offshore and near-shore environments. Large research efforts in recent years have substantially increased our knowledge of large- and medium-scale submarine slope instabilities (Locat & Lee, 2000). Numerous

examples of submarine landslides have been documented, most of them along open continental slopes (e.g. Kenyon, 1987; Piper *et al.*, 1999; Imbo *et al.*, 2003), in submarine canyons (e.g. Carlson & Karl, 1988) and river deltas (e.g. Prior & Coleman, 1978). In fjords and fjord-type lakes, the studies have mainly concentrated on headwall deltas (Prior *et al.*, 1984; Shilts & Clague, 1992) and side-entry deltas (Terzaghi, 1956; Prior *et al.*, 1981). Although the steep lateral non-delta slopes of perialpine lakes and fjords are often covered with sedimentary drapes that are susceptible to sliding, corresponding mass movements have only been briefly mentioned in the literature (e.g. Giovanoli *et al.*, 1984; Chapron *et al.*, 1996; Syvitski & Schafer, 1996; Eyles *et al.*, 2000) and detailed case studies (e.g. Kelts, 1978; Kelts & Hsü, 1980) are rare.

Sharp breaks between steep lateral slopes and intervening flat lake basin floors are peculiar characteristics of perialpine lakes and fjords. This geometry strongly influences the flow behaviour and depositional characteristics of lateral mass movements (Komar, 1971; Kelts & Hsü, 1980; Nemec, 1990) and favours compression and deformation of the flat-lying, lake-floor sediments through the impact and load of the descending masses (Syvitski & Schafer, 1996). Although such deformation can be extensive, the processes involved are poorly understood.

In this study, redepositional processes in lakes are linked to the sedimentary features observed in the resultant deposits. The characteristics of four lateral slides, of different scale, in Lake Lucerne, Central Switzerland (Fig. 1A), are described. The architecture of the failure scars, mass-movement deposits and deformed basin-plain sediments were imaged by means of high-resolution seismic reflection profiling and evaluated with piston coring. Based on these observations, the slide history and the processes governing the mass-movement evolution are reconstructed. In particular, special attention is given to the deformation of basin-plain sediment by the loading of the basin floor by descending masses.

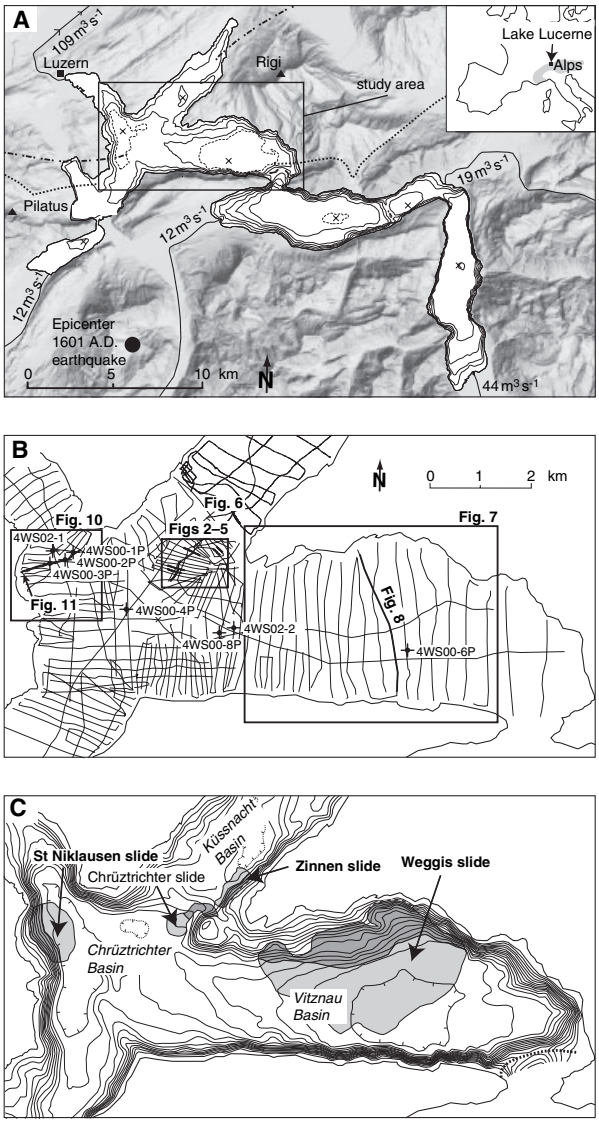

Fig. 1. (A) Geological and hydrological setting of Lake Lucerne. The dotted and dashed-dotted lines mark the alpine and the subalpine front respectively. These two major thrusts separate, from south to north, the Helvetic Nappes, the Subalpine Molasse and the Plateau Molasse. Bathymetric contour interval is 40 m with crosses marking the deepest points of the seven basins of the lake. Dotted contour lines represent 20 m intervals and aim to clarify the bathymetry. (B) 3·5 kHz seismic survey grid and locations of piston cores. Rectangles and bold lines indicate the position of maps and seismic profiles presented in subsequent figures. (C) Bathymetry of the three studied basins as derived from the seismic data. Contour interval is 10 and 5 m for solid and dotted lines respectively. The bold dotted line indicates a major subaqueous sill. Slide complexes discussed in this paper are marked with grey shadings, whereby dark and light grey indicate dominant erosional and depositional zones respectively.

Mass-movement terminology

The mass-movement terminology used in this paper is based on the seismic signature of the sediments. Failure scars, slide deposits, massflow deposits and large turbidites are typical mass-movement features that can be recognized on seismic sections. Note that, as a result of successive disintegration and water-incorporation

during descent, a mass movement generally transforms from a coherent slide block with a distinct sliding plain into a massflow and finally into a turbidity current (e.g. Mulder & Cochonat, 1996 and references therein). Consequently, a single mass-movement event usually produces more than one type of deposit.

Slides leave distinct failure scars and gliding planes on the subaqueous slopes. Slide deposits show contorted or faulted, but essentially continuous reflections on seismic sections because the internal structure of the redeposited material remains largely undisturbed and displacement is limited (Nardin *et al.*, 1979; Mulder & Cochonat, 1996). In this study, the term slide is not only used for the initial, up-dip phase of a mass movement, but also to name the entire 'slide-flow-turbidite complex' (e.g. 'Vitznau Slide').

Massflow deposits generally occur at the toe of slopes and build up sediment wedges with a chaotic-to-transparent seismic facies, irregular lower surfaces that crosscut stratigraphy, slightly hummocky to fairly smooth upper surfaces and distinct distal terminations (e.g. Prior *et al.*, 1984). Such characteristics indicate a lack of large coherent blocks reflecting a higher degree of remoulding and disintegration of massflow compared with slide deposits.

Turbidites related to massflows generally appear as confined bodies in the deepest part of the basins and show an almost transparent seismic facies with smooth upper surfaces. These bodies often directly overlay the massflow deposits to which they relate. The transparent seismic facies of such turbidites is the result of their relatively homogeneous nature. Compared with flood-related turbidites, turbidites related to medium to large massflows are generally thicker with much larger volumes. Besides the sediment brought into suspension directly from the massflow, such turbidites often include material lofted by tsunamis or seiches. As a consequence of their complex and diverse evolution, such deposits have been named 'seismoturbidite' (Nakajima & Kanai, 2000), 'seiche deposits' (Siegenthaler *et al.*, 1987; Van Rensbergen *et al.*, 1999), 'homogenite' (Kastens & Cita, 1981; Siegenthaler *et al.*, 1987; Chapron *et al.*, 1999) and 'megaturbidite' (Bouma, 1987). As the described turbidite bodies are usually a coalescing product of different processes, the purely process-oriented names 'seismoturbidite' and 'seiche deposits' are avoided here. In addition, the term 'homogenite' is inappropriate as the relevant beds in Lake Lucerne are not completely homogeneous but typically show a graded base. Consequently, the widely accepted and more general term 'megaturbidite' (Bouma, 1987) is used. Note that the term 'mega-' refers to the unusual size of the turbidites compared with other, mostly flood-generated turbidites in the same setting. Consequently, megaturbidites in a lake are relatively small compared with their oceanic counterparts.

METHODS

Selected basins of Lake Lucerne were surveyed using a high-resolution, single-channel seismic system with a centre frequency of 3·5 kHz (pinger source). The source/receiver was mounted on a cataraft that was pushed by a vessel. Differential GPS provided a horizontal positional accuracy of ±2 m. The studied basins were covered with a dense grid of more than 300 km of seismic lines revealing a quasi-3D image of the subsurface.

Data processing was carried out with SPW™ software (Parallel Geoscience Corp., Incline Village, NV, USA) and included band pass filtering, automatic gain control, spiking deconvolution and muting of the noise in the water column. No migration was applied to the data. Water depths were calculated assuming a velocity of 1500 m sec^{-1}. The bathymetric maps shown in this paper are based on the seismic data.

Sediment cores were retrieved using a Kullenberg-type piston corer (Kelts *et al.*, 1986). Gamma-ray attenuation bulk density, magnetic susceptibility and P-wave velocity were measured on whole-round cores with a GEOTEK™ (GEOTEK Ltd, Daventry, UK) multisensor core logger. Subsequently, the cores were split, photographed and described macroscopically. Core-to-core correlation was achieved by comparing both visual characteristics and petrophysical properties. Bulk density and P-wave velocity profiles enabled an accurate seismic-to-core correlation.

Sedimentation in Lake Lucerne

Lake Lucerne is a perialpine lake of glacial origin situated in Central Switzerland. It has a total surface area of 116 km^2 and consists of seven steep-sided basins with flat bottoms (Fig. 1A). Four major alpine rivers feed the internal four basins providing approximately 80% of the lake's water supply. This study concentrates on the three external basins (the Chrüztrichter, Vitznau and Küssnacht basins) that are separated from the major deltas by subaqueous sills. All of the slides

discussed are located north of the alpine front, in areas with a molassic substratum mainly consisting of sandstones and conglomerates.

In the central part of the Vitznau Basin the bedrock is covered with a 117 m thick glaciolacustrine infill (Finckh *et al.*, 1984). Seismic stratigraphy calibrated with piston coring and radiocarbon dating indicates that most of these sediments were deposited during the Late Glacial period and only the uppermost 5–15 m are of Holocene age (Schnellmann, 2004). Whereas Late Glacial sedimentation was focused in topographic depressions, the Holocene sediments are more widely and regularly distributed and also drape the sub-lacustrine slopes. Similar observations in other perialpine lakes have been interpreted as reflecting a major change in the sedimentary system. Whereas in Late Glacial times most of the sediment was deposited on deltas and in the deep basins by underflows, the increasing importance of interflows and authigenic production during the Holocene led to a more regularly distributed sedimentation with increased accumulation of fine grained sediment even on relatively steep marginal slopes (Sturm & Matter, 1978; Mullins *et al.*, 1991; Van Rensbergen *et al.*, 1999; Eyles *et al.*, 2000; Beck *et al.*, 2001).

Piston cores from areas with rather condensed Holocene sedimentary sequences reached the uppermost 1–5 m of the Late Glacial basin fill (cores 4WS00-4P, 4WS00-8P, 4WS02-1, 4WS02-2 in Fig. 1B; Schnellmann, 2004). These deposits comprise grey to yellowish mud with a very fine, most probably annual lamination (glacial varves) and frequent intercalated graded beds of brown, grey and beige colour (turbidites). The Holocene sediments consist of faintly laminated, grey to brown mud with dark layers rich in organic matter (mainly leaves and debris of land plants) and some intercalated, mm- to few cm-thick graded layers of beige, brown or grey (turbidites).

Numerous failure scars, massflow deposits and megaturbidites can be recognized on seismic sections through the studied lake basins. The massflow deposits observed range in thickness from <1 to >10 m and occur either at the foot of subaqueous slopes with inclinations >10° or in front of rockfall cones. Systematic seismic-stratigraphic mapping and correlation of the massflow deposits identified in the study area shows that the majority of these deposits are no single incidents, but belong to, most probably earthquake-triggered, multiple events (Schnellmann *et al.*, 2002; Schnellmann, 2004).

In the following, the detailed characteristics of subaqueous mass-movement deposits in Lake Lucerne are pointed out based on four case studies of different scale. The first three examples described (Chrüztrichter, Zinnen and Weggis slides; Fig. 1C) are part of a multiple-slide event triggered by the historically well-documented 1601 AD, magnitude ≈6·2 earthquake (Fäh *et al.*, 2003; Schwarz-Zanetti *et al.*, 2003). The last case study (St Niklausen Slide; Fig. 1C) belongs to a prehistoric earthquake-triggered multiple-slide event ^{14}C-dated to 2420 cal yr BP (Schnellmann *et al.*, 2002).

CASE STUDIES

Chrüztrichter Slide

The relatively small Chrüztrichter Slide is located on the north-western edge of the Chrüztrichter Basin and affects an area of 0·3 km^2 from failure scar to toe of deposits (Figs 1C and 2). The failure scar lies on a 10–15° steep, northward-dipping slope of a small subaqueous mound at 30–40 m water depth. It cuts a 5–6 m thick, acoustically laminated sedimentary drape that overlies acoustic basement in the undisturbed slope environ-

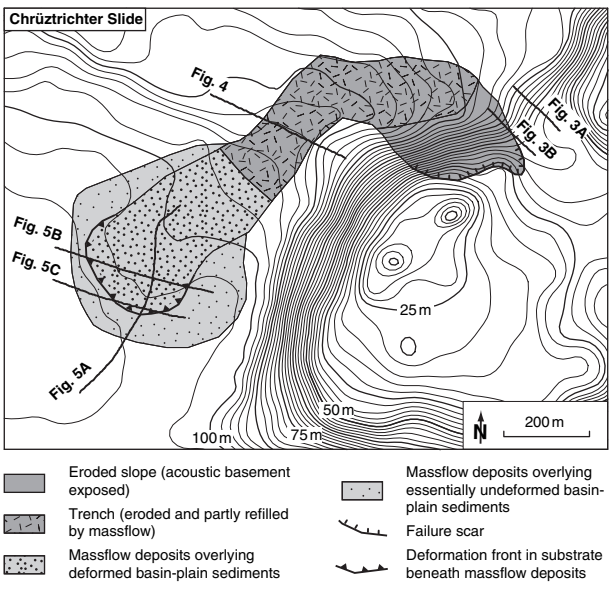

Fig. 2. Bathymetric map of the Chrüztrichter Slide area. Contour interval is 2·5 m. Dark and light grey shadings outline the erosional and depositional zones of the slide respectively. Both bathymetry and outline of the four different slide provinces are based on the dense grid of 3·5 kHz seismic lines shown in Fig. 1B. See Fig. 1B for wider location within Lake Lucerne.

ment above and lateral to the failure scar (Fig. 3). The absence of the entire drape points towards a translational slide with the acoustic basement acting as the failure surface.

The pathway of the slide and the massflow it transformed to is marked by a counterclockwise rotation from a northward to a south-westward-directed movement, following the steepest topographic gradient (Fig. 2). At its central part, the pathway narrows as a result of basement-controlled bathymetric constriction, and a 150 m wide trench is cut into acoustically laminated lake sediments, most probably as a result of increased flow velocities in this bottleneck area (Fig. 4; Gee *et al.*, 2001). The erosive trench is partly filled with massflow deposits imaged on the seismic section by a package of chaotic-to-transparent seismic facies with a flat, rather smooth upper surface. The acoustically chaotic-to-transparent deposits forming a tiny bulge above the north-western rim of the trench are interpreted as the result of material overflowing the trench margins during passage of the massflow.

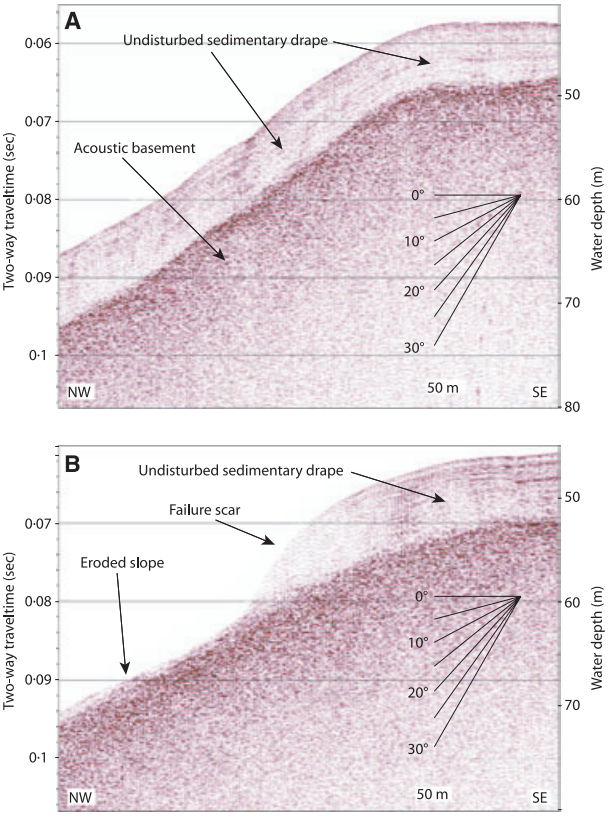

Fig. 3. Two parallel 3·5 kHz seismic lines across the sub-lacustrine slope in the vicinity of the headwall of the Chrüztrichter Slide. The distance between the lines is about 80 m. For exact location see Fig. 2. (A) Profile shows the undisturbed slope outside the area of slope failure characterized by an approximately 6 m thick continuous sedimentary drape directly overlying acoustic basement. (B) Profile across slide scarp showing slope that is eroded down to the acoustic basement. The rather diffuse appearance of the failure scar is interpreted as a result of the oblique orientation of the seismic line relative to the slide axis.

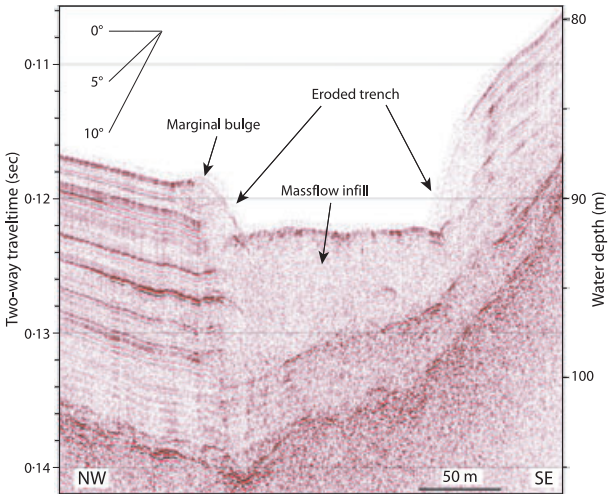

Fig. 4. A 3·5 kHz seismic line across the central bottleneck area of Chrüztrichter Slide showing a 150 m wide, eroded trench. It is partly refilled by massflow deposits with a chaotic-to-transparent seismic facies and a fairly smooth top. The location of the line is given in Fig. 2. The tiny topographic bulge at the north-western rim of the trench is interpreted as the result of an overflow of the trench margins during massflow passage.

A positive relief feature at the mouth of the trench indicates a depositional lobe at the edge of the basin plain (Fig. 2). Figure 5A shows a longitudinal line, whereas Fig. 5B and C shows two slightly oblique cross-sections through the frontal part of this lobe. Continuous reflections indicate undisturbed sedimentary layering in the lowermost part of these profiles. Further above, acoustically laminated sediment packages are deformed and displaced relative to each other and form a soft-sediment fold-and-thrust belt. Deformation is concentrated in distinct shear zones between undisturbed sediment blocks. Comparison of the seismic reflection patterns of different, acoustically layered packages reveals reverse faults with vertical offsets of up to 3 m. Duplicated sedimentary units indicate major thrusting. A profile trending perpendicular to the main axis of the deposits shows thrust systems verging in opposite directions, a phenomenon that is obviously related to the semicircular deformation front (Figs 2 and 5B). This curvilinear nature of the deformation front indicates that radial forces induced the deformation. The thrust front is expressed by a blind thrust that

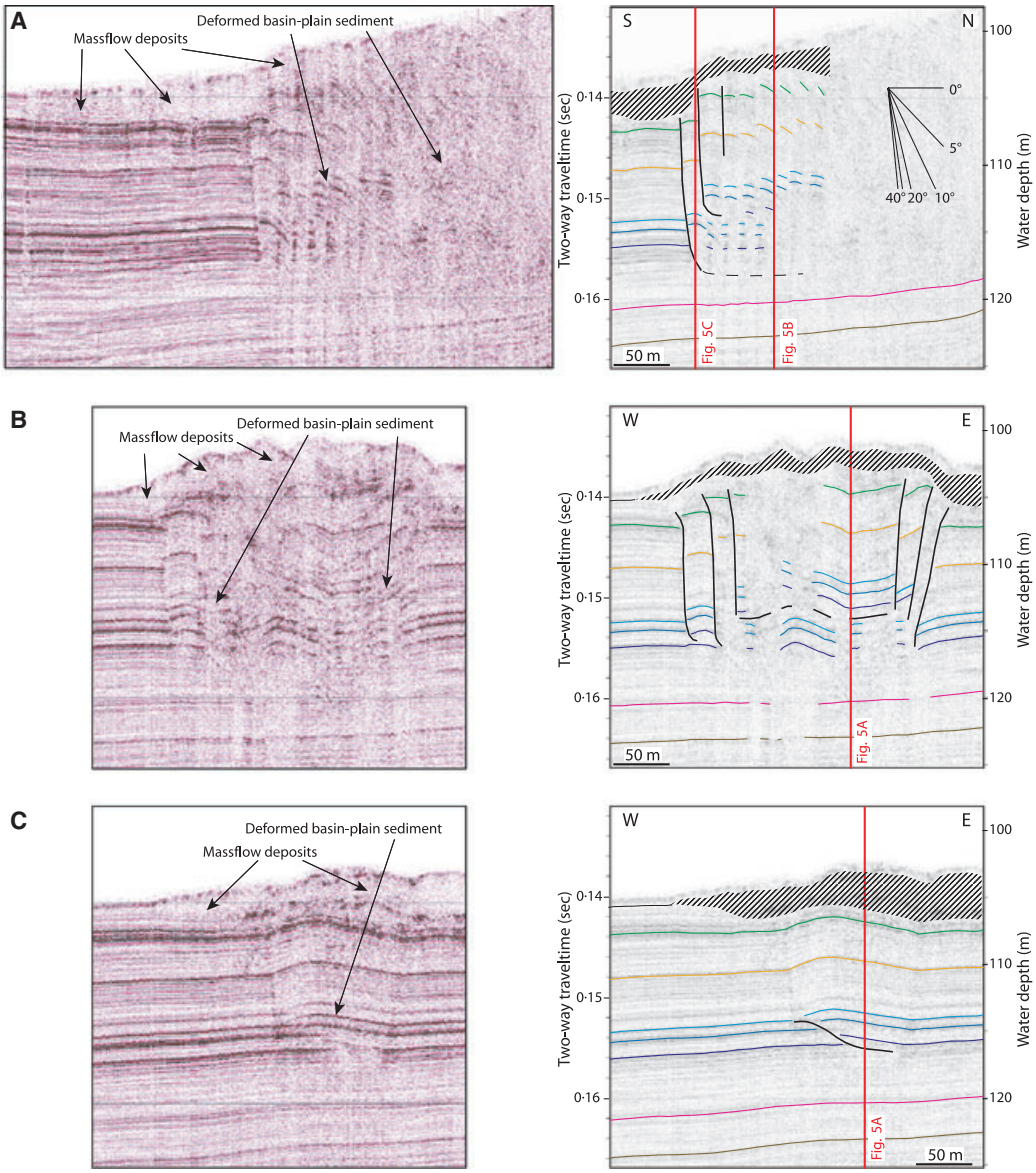

Fig. 5. Three 3·5 kHz seismic lines imaging the depositional zone of the Chrüztrichter Slide. Whereas the line displayed in (A) is approximately parallel to the movement direction of the slide, the profiles shown in (B) and (C) represent slightly oblique cross-sections. The locations of the lines are indicated in Fig. 2. Interpretations are given on separate panels on the right-hand side. Coloured lines mark seismic stratigraphic horizons, whereas black lines denote faults. Hatched surfaces are interpreted as massflow deposits. Vertical red lines indicate intersections between the individual seismic sections.

detaches at ≈12 m sediment depth (Fig. 5C). Towards the more internal, northern part of the deformed zone, acoustically layered blocks become smaller and less frequent and the seismic facies grades into a chaotic-to-transparent type. In this northern zone, deformation and remoulding of the sediment seem to be more intense and, as a result, the remaining undisturbed sediment blocks become too small to be imaged by the limited horizontal resolution of the seismic system (Fig. 5A).

The uppermost part of the depositional lobe consists of an up to 2 m thick package of massflow deposits characterized by a chaotic-to-transparent seismic facies and distinct frontal and lateral terminations (Fig. 5). The post-massflow cover is less than a few dm thick. However, its exact thickness is difficult to determine because of the strong seismic lake floor signature.

Massflows and/or related water movements often loft suspension clouds and thereby initiate

turbidity currents. In the case of the Chrüztrichter Slide, no evidence for a massflow-related turbidite can be seen on seismic sections, despite the existence of a small depression adjacent to the depositional lobe (Fig. 1C), which could potentially trap a turbidity current.

Zinnen Slide

This small slide (≈0·25 km^2) is located in the southern part of the Küssnacht Basin (Fig. 1C), in an area characterized by a sharp break between the steep slope (≈15°) and the flat basin plain. An approximately 2 m high failure scar is located at 30–40 m water depth. Beneath the failure scar the acoustic basement is exposed.

A sediment wedge with a primarily chaotic-to-transparent acoustic signature is present along the edge of the 73 m deep basin plain (Fig. 6). Close to the slope break, the chaotic-to-transparent seismic facies extends down to a sediment depth of 8–12 m. Further basinwards, a thin sheet of massflow deposits overlie acoustically layered sediment. A ramp anticline with an associated backthrust, as well as several minor reverse faults, can be seen in the acoustically laminated sediments below the internal part of the thin massflow sheet (Fig. 6). The décollement of these deformation structures is located at 8 m sediment depth in an area characterized by high-amplitude reflections. At the lake floor the ramp anticline is expressed by a bulge, indicating folding and thrusting of the overridden basin-plain sediments during and/or just after emplacement of the massflow deposits. The post-event sediments covering the massflow deposits are maximally a few dm thick.

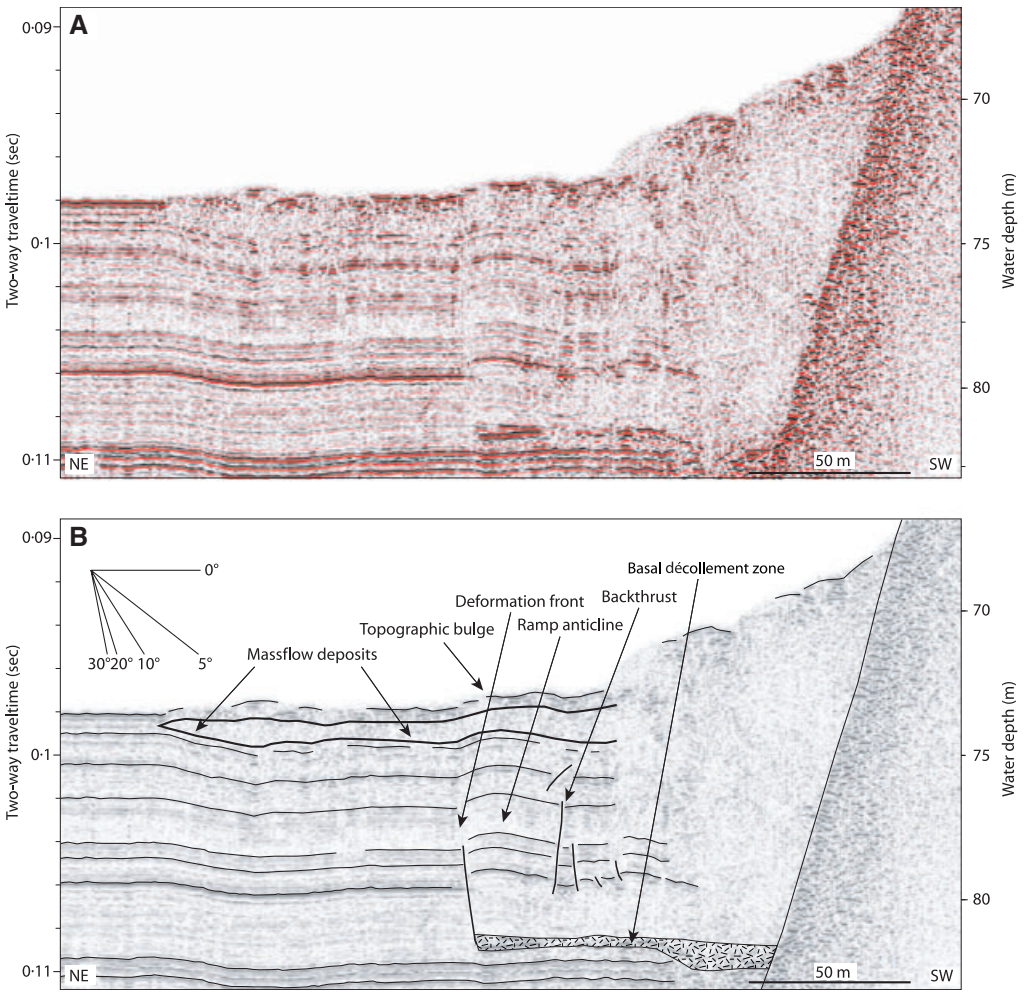

Fig. 6. Uninterpreted (A) and interpreted (B) 3·5 kHz seismic lines across the deposits of the Zinnen Slide. The location of the profile is indicated in Fig. 1B. Note the slight bulge in the lake floor directly above the blind thrust. It indicates thrust emplacement during and/or just after massflow deposition.

Weggis Slide

The biggest slide in the study area, the Weggis Slide, is located on the northern slope of the Vitznau Basin (Figs 1C and 7) and affects an area of about 6·5 km^2. At the time of its discovery, it was interpreted as the subaqueous continuation of a subaerial earthflow (Hsü & Kelts, 1985). This event took place in 1795 AD, lasted 2 weeks and destroyed 33 buildings in the village of Weggis. Later, it was shown that the subaqueous deposits are older than this earthflow event and relate to the 1601 AD, magnitude ≈6·2 earthquake (Siegenthaler *et al.*, 1987; Lemcke, 1992).

Whereas the southern slope of the Vitznau Basin consists of a steep rock face, the northern slope is flatter and shows a more irregular bathymetry with two topographic steps and an intermediate terrace (Figs 7 and 8A). The sedimentary infill of the central basin consists mainly of flat-lying, acoustically layered sediment. In contrast, material that was transported or deformed by the slide shows a characteristic chaotic-to-transparent acoustic signature (Fig. 8A).

The failure scar reaches a maximum height of 6 m and extends laterally over more than 6 km in water depths ranging from 40 to 100 m (Fig. 7). In the area of Weggis, the depth of the scar cannot be determined because of the overprint of the 1795 AD earthflow event mentioned above. In Fig. 8A, the failure scar appears at ≈45 m water depth in a zone where the slope inclination increases downwards from <10° to 15°.

Seismically chaotic-to-transparent zones indicate slide and massflow deposits on a subaqueous terrace and in the basin plain. In the central part of the basin, these deposits are wedge-shaped and overlie acoustically stratified and, therefore, undisturbed basin-plain sediment (Fig. 8B). Towards the northern basin edge, this acoustic stratification ends abruptly and grades into a chaotic-to-transparent seismic facies, indicating deep-reaching deformation of the slope-adjacent basin-plain sediment. Figure 8C shows a close up of this seismic facies boundary, separating disturbed from undisturbed basin-plain sediment. Within the chaotic-to-transparent seismic zone, some packages with intact acoustic layering are

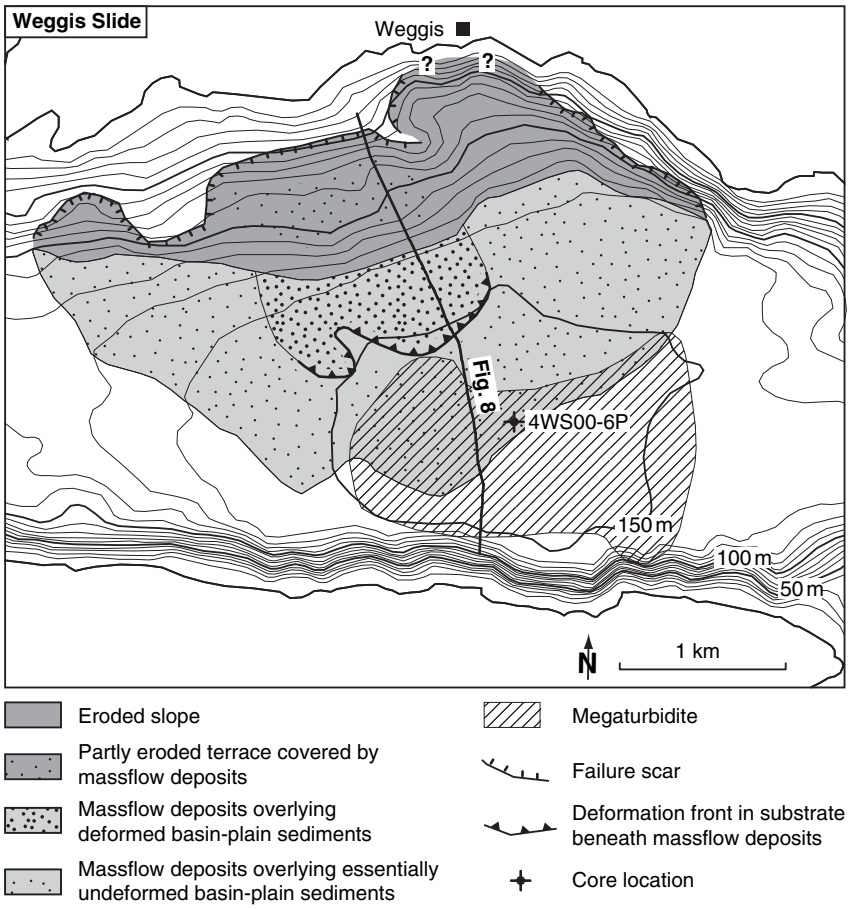

Fig. 7. Map of the Vitznau Basin showing the outline of the Weggis Slide. Contour interval is 10 m. See Fig. 1B for location of the map segment.

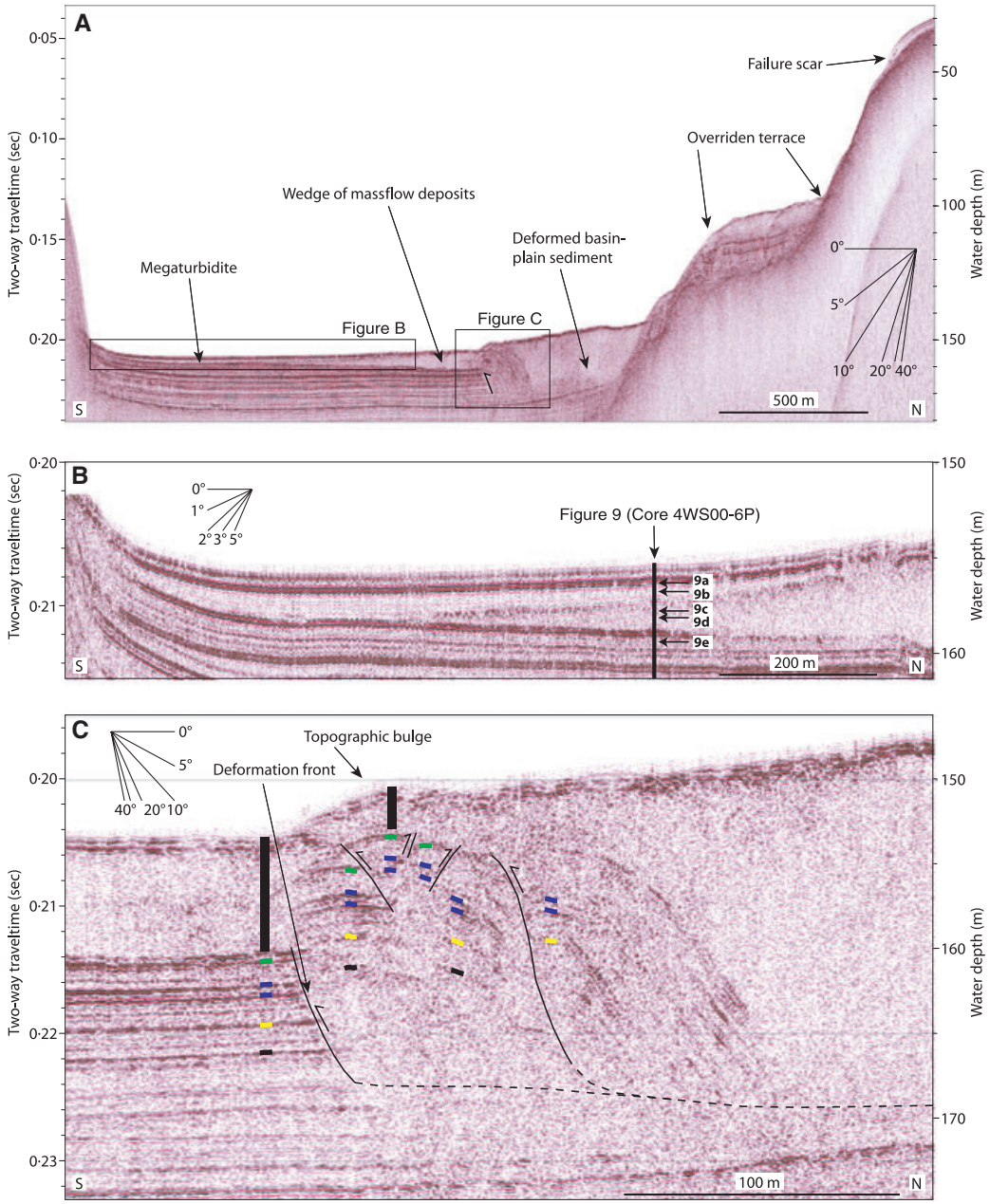

Fig. 8. A 3·5 kHz seismic line illustrating the structure of the Weggis Slide. (A) Seismic profile showing the morphology of the Vitznau Basin and the acoustic signature of its sedimentary infill. (B) Enlargement of seismic line (A) showing distal massflow wedge and overlying contained megaturbidite. (C) Enlargement of line (A) showing the boundary between deformed and almost undeformed basin-plain sediment. Black lines denote faults, coloured bars mark specific seismic stratigraphic horizons. Note the major frontal thrust with a vertical offset of about 5 m and the overlying slight bulge in topography. The deposits overlying the green seismic stratigraphic horizon (indicated by a vertical black bar) are thicker in the footwall than in the hangingwall, indicating syndepositional thrust emplacement.

present. A comparison of the reflection patterns of these packages reveals a major frontal thrust with a vertical offset of 4–5 m. A second, more internal thrust package is faintly recognizable further to the north. The décollement of these structures presumably lies 15–20 m below the lake floor, as the deeper sediments show an undisturbed acoustic layering. Mapping of the deformation front reveals two semicircular structures that project out 600 m into the basin plain (Fig. 7).

Concerning the timing of basin-plain deformation, two observations from Fig. 8C are partic-

ularly relevant: (1) the frontal thrust is clearly expressed at the lake floor by a topographic bulge; and (2) the thickness of the sediment overlying the green seismic stratigraphic horizon (vertical black bar in Fig. 8C) is 7 and 3 m in the footwall and the hangingwall respectively. The existence of a topographic bulge related to the frontal thrust shows that the thrusting does not predate the emplacement of the massflow deposits, as otherwise the latter would have levelled out the topography to a high degree. Neither can the thrust be purely 'post-massflow', because then, the thicknesses of the deposits overlying the green seismic-stratigraphic horizon should be the same in the hanging and in the footwall. Consequently, thrusting must essentially have taken place during massflow deposition.

Distally, a wedge of massflow deposits with a chaotic-to-transparent seismic facies and a relatively smooth upper surface overlies almost undisturbed basin-plain sediment showing a continuous acoustic layering (Fig. 8B). The wedge is directly superimposed by an up to 2 m thick, acoustically transparent body that shows a smooth surface and appears focused in the deepest part of the basin levelling out the bathymetry. This sedimentary body is interpreted as massflow-related megaturbidite, based on its seismic facies and geometry, as well as its stratigraphic position directly on top of the massflow deposits. It is covered with a few dm of acoustically layered, post-event sediments.

Figure 9 shows photographs of a piston core through the distal part of the Vitznau basin and includes undisturbed sediments as well as massflow and megaturbidite deposits related to the Vitznau Slide. The undisturbed sediments consist of faintly laminated mud intercalated with black, organic carbon-rich layers and brown to beige, graded turbidite beds (Fig. 9A and E). The massflow-related megaturbidite consists of homogeneous grey mud with a graded, silty to sandy base and a characteristic thin, light-grey clayey cap (Fig. 9A and B). Whereas the uppermost part of the massflow deposits is highly disintegrated and consists of a conglomerate of small mudclasts (Fig. 9C), larger clasts of partly folded strata are abundant further below (Fig. 9D).

St Niklausen Slide

Affecting an area of 0·8 km^2 from failure scar to toe of massflow deposits, the St Niklausen Slide complex is of medium size compared with the case studies presented above. The studied slope is located in the western Chrüztrichter Basin (Figs 1C and 10) and has repeatedly become unstable in Late Glacial and Holocene times, as indicated by stacked massflow deposits on the basin plain (Fig. 11). A 1·5 km long and up to 6 m high failure scar is located on a downwards steepening slope at 40–50 m water depth (Fig. 11). On a 10–20° steep section of the slope, the acoustic basement is covered only by post-event sediment (Fig. 11).

The following description will concentrate on the most recent massflow deposit. It was dated at 2420 cal yr BP and is part of a multiple mass-movement event described further in Schnellmann *et al.* (2002). The distal part of the massflow lobe is composed of a thin sheet of sediments with a chaotic-to-transparent seismic facies (Fig. 12A). It overlies almost undisturbed, basin-plain sediments characterized by continuous reflections on seismic sections. Closer to the western basin margin slope, these reflections

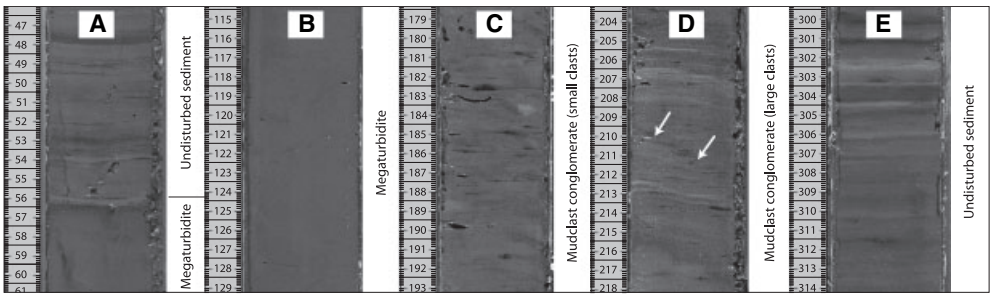

Fig. 9. Core photographs showing the distal deposits of the Weggis Slide complex (core 4WS00-6P). The core location is shown in Fig. 7 and is indicated on the seismic section displayed in Fig. 8B, with arrows marking the position of the individual core photographs. (A) Uppermost part of the megaturbidite and the overlying post-event sediments. (B) Homogeneous megaturbidite. (C, D) Massflow deposits consisting of conglomerate with small mudclasts and larger pieces of intact strata. White arrows in (D) indicate a shear zone separating two large clasts. (E) Regular sediments underlying the massflow deposits.

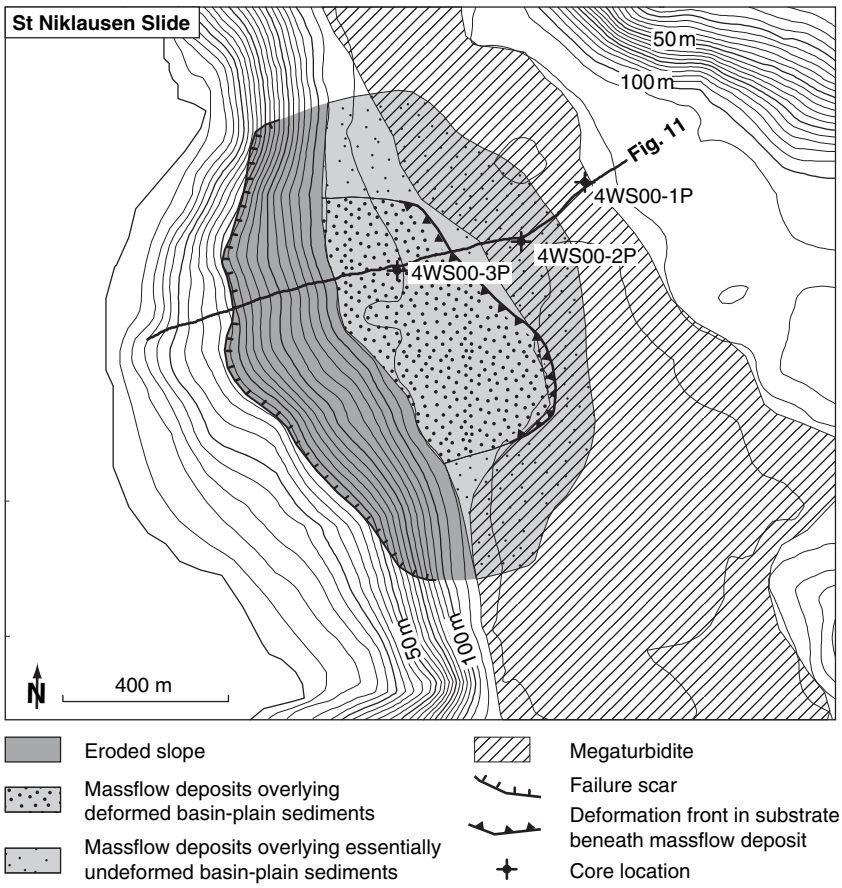

Fig. 10. Bathymetric map with the outline of the St Niklausen Slide. Contour interval is 5 m. For location of the map segment shown, see Fig. 1B.

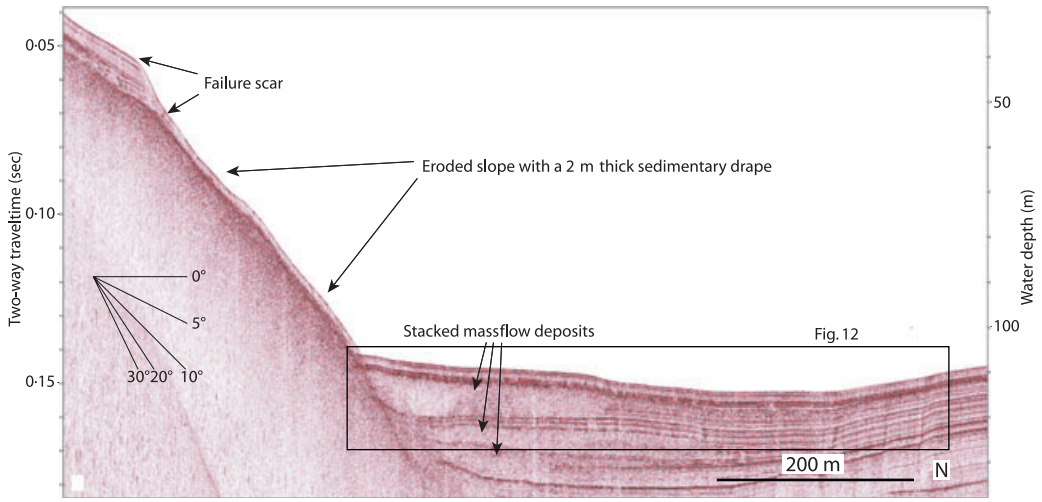

Fig. 11. A 3·5 kHz seismic section through the area of the St Niklausen Slide. The location of the line is indicated in Fig. 10. Note the position of the failure scar in a zone with lakeward-increasing slope angle. Stacked massflow deposits in the slope-adjacent basin-plain sediments indicate repeated sliding on the same slope. Note the recent sedimentary drape covering the slope.

end abruptly and border a 6–8 m thick package of acoustically chaotic-to-transparent sediment. The sharp and steep lateral seismic facies boundary is interpreted as deformation front separating deeply deformed from essentially undeformed basin-plain sediment. A bulge in topography, which directly overlies this deformation front, points towards a major frontal thrust. In contrast

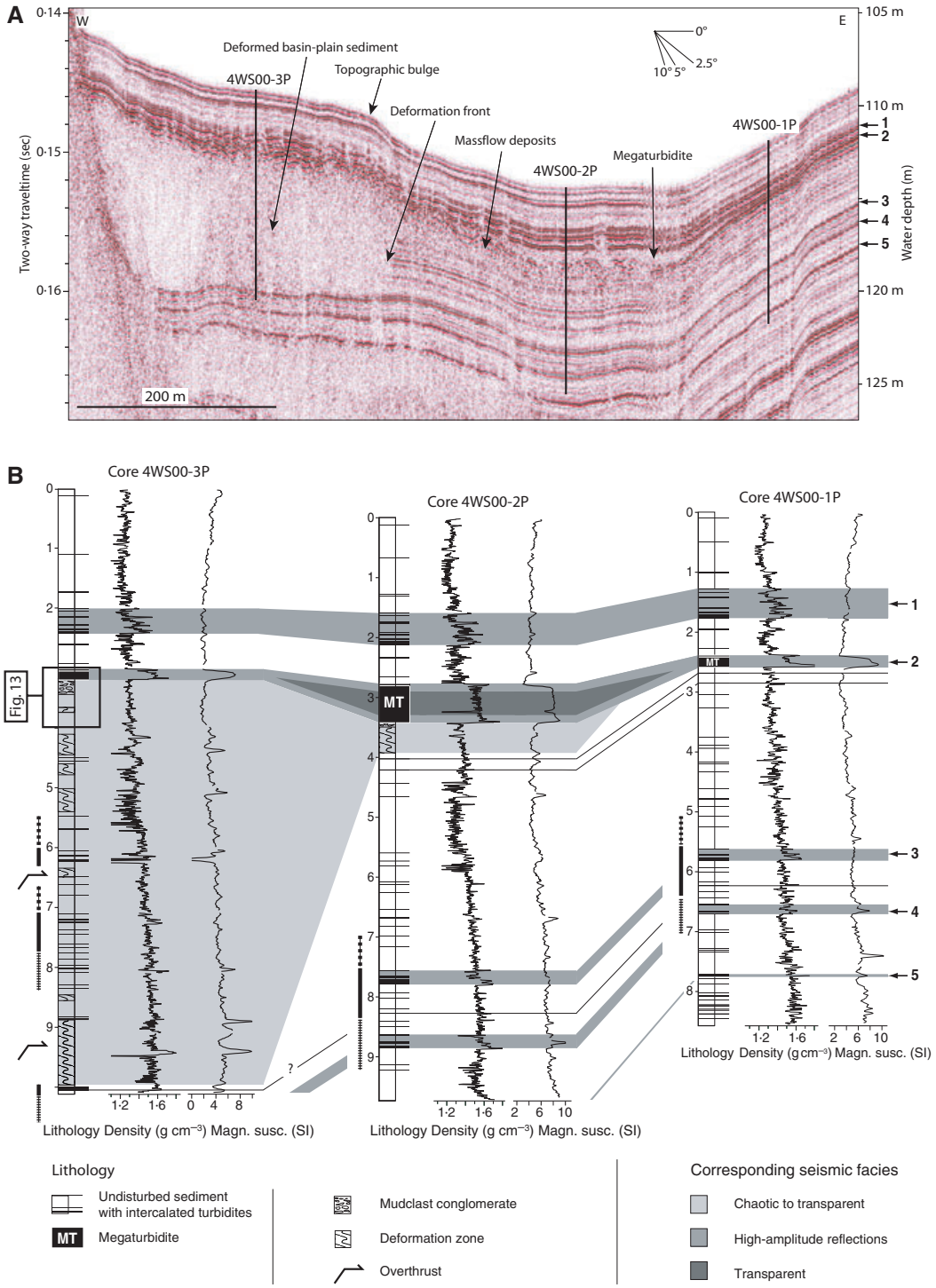

to previous examples, the seismic facies changes directly from a chaotic-to-transparent type to an acoustically layered type, and a transition zone with displaced, acoustically laminated sediment blocks is absent. Here, internally undisturbed sediment blocks may be too small to be imaged by the seismic system. An acoustically almost transparent body that is restricted to the deepest part of the basin and directly superimposes the massflow deposits, is interpreted as megaturbidite.

In order to gain insight into the internal sediment structures of the acoustically chaotic-to-transparent zone, three 8–10 m long piston cores were retrieved along the axis of the slide complex, through slope-adjacent massflow deposits with deformed substrate, through more distal

Fig. 12. (A) Close up from the seismic section of Fig. 11 showing the deposits of the most recent slide in the St Niklausen area, ^{14}C dated at 2420 cal yr BP (Schnellmann *et al.*, 2002). Three different zones can be seen: (i) a slope-adjacent zone characterized by deep reaching, basin-plain deformation; (ii) a central basinal zone with a thin massflow package overlying almost undisturbed basin-plain sediment; and (iii) a distal zone beyond the reach of the massflow with an eastward thinning, contained megaturbidite. (B) Lithology, gamma-ray attenuation bulk density and magnetic susceptibility logs for three piston cores retrieved from these deposits. Data points from section ends were removed in the density and magnetic susceptibility logs because end caps did not allow proper measurement procedure. The location of the cores is denoted in (A) as well as on the map shown in Fig. 10. Seismic-to-core correlation is indicated by five numbered arrows at the right hand side of (A) and (B). The strong reflections in (A) are interpreted as a response of the zones with high-density contrasts outlined by grey bars in (B). The sediment retrieved from the acoustically chaotic-to-transparent zone (core 4WS00-3P) is characterized by up to 2 m thick, undisturbed sediment blocks that are separated by relatively small deformation zones. Repeated sedimentary sections and two major overthrusts are indicated on the left-hand side of the core log by bars (dotted, solid and dashed) and arrows respectively. The identification of these repeated sequences is based on core-to-core correlation and ^{14}C dating (Schnellmann, 2004). Core-to-core correlation of cores 4WS00-2P and 4WS00-1P indicates that the full stratigraphic succession is present in both these cores. Consequently, the ≈0·5 m thick massflow deposits present in core 4WS00-2P must have been deposited without significant erosion or deformation of the underlying basin-plain sediments.

massflow deposits with undeformed substrate and through undisturbed sediments respectively (Figs 10 and 12). Figure 12B shows lithology, density and magnetic susceptibility logs of the three cores. Numbered arrows on the right-hand side of Fig. 12A and B indicate prominent reflections and their seismic-to-core correlation.

The lower part of the slope-adjacent deposits (core 4WS00-3P) is characterized by faintly layered, up to 1·5 m thick undisturbed sediment blocks that are separated by shear zones consisting of folded and disrupted sediment. Two major overthrusts and associated repeated sediment packages are indicated in Fig. 12B. The highly deformed base of the deformation zone at 9–10 m in core 4WS00-3P presumably represents the main thrust décollement. Whereas undisturbed sediment blocks reach thicknesses >1·5 m in the central part of the deformed zone, the size of these blocks decreases towards the top, where deformation becomes more intense. The uppermost 25 cm of the disturbed zone consists of a mudclast conglomerate indicating extensive remoulding and disintegration of the sediments during transport. This zone is directly overlain by a 12 cm thick megaturbidite consisting of grey to brown silty clays with a graded sandy base and a light-grey clayey cap. The core photograph in Fig. 13 shows the three main types of redeposited and deformed sediment described above: (i) undisturbed sediment blocks separated by deformation zones; (ii) mudclast conglomerate; and (iii) megaturbidite.

In a more distal position of the massflow lobe, mudclast conglomerates and deformed sediment are restricted to a 0·5 m thick zone (core 4WS00-2P). Core-to-core correlations show that further below the complete and undisturbed stratigraphic succession is in place. Consequently, the 0·5 m thick zone is interpreted as the product of a massflow, which neither removed nor deformed substantial parts of the substrate during emplacement.

DISCUSSION

In the following section the four studied mass-movement complexes are compared. The dynamics of the slides, massflows and related turbidity currents are discussed separately, before the deformation of the basin-plain loaded by slide and massflow is considered.

Initial slide failure

A major precondition for sliding is the availability of sediment on the slope. As in many perialpine lakes (e.g. Van Rensbergen *et al.*, 1999; Eyles *et al.*, 2000), a primarily Holocene drape covers large parts of Lake Lucerne. No, or very little, sediment accumulation is seen on seismic sections on very steep slopes and cliffs only. In the four examples presented, the whole sedimentary drape slid away as a translational slide (Mulder & Cochonat, 1996) that made a detachment located at the top of the acoustic basement.

The geometry and position of failure scars contain information about possible triggering mechanisms (Mulder & Cochonat, 1996). As the failure scars of the slides discussed mostly lie in water depths >30 m, surface waves and human activity can be excluded as triggering mechanisms. Moreover, the considerable depth of the scars implies that the slides do not represent the subaqueous continuations of subaerial mass

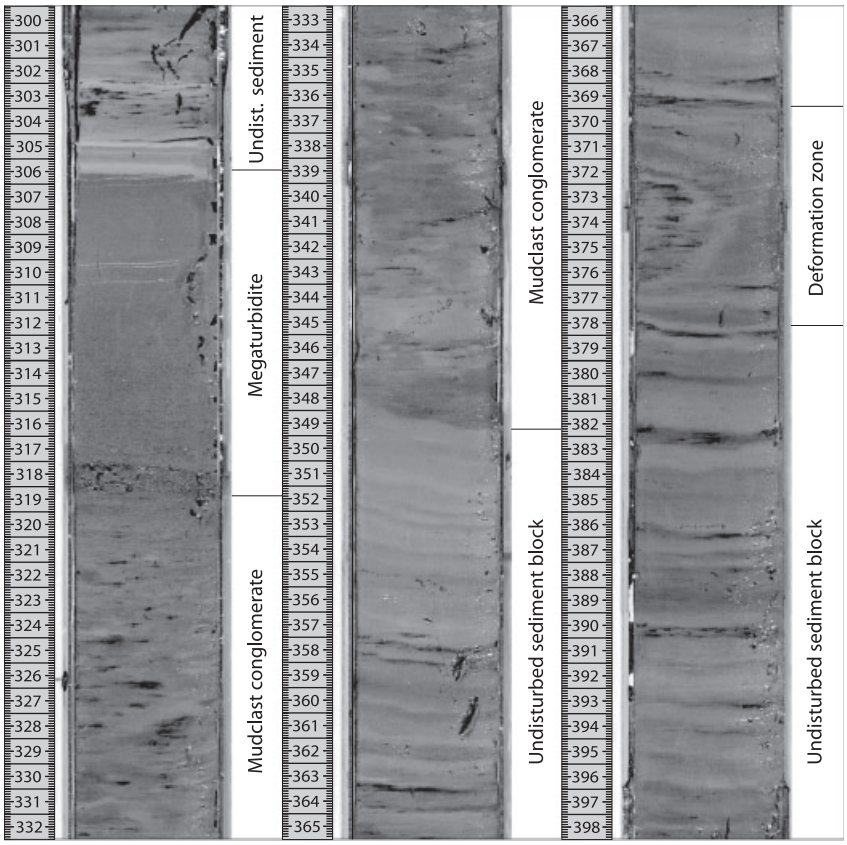

Fig. 13. Photograph of core 4WS00-3P, which recovered the massflow deposits of the St Niklausen Slide and underlying deformed basin-plain sediment. Position of the core segment shown is denoted on the lithological log in Fig. 12B. The megaturbidite and the mudclast conglomerate deposits in the upper part of the core photograph (3·05–3·48 m core depth) are characterized by a relatively high degree of disintegration. Further below, deformation is concentrated in relatively narrow shear zones between undisturbed sediment blocks.

movements. This is in agreement with earlier work, which related the Weggis, Chrüztrichter, Zinnen and St Niklausen slides to multiple-slide events triggered by strong historic and prehistoric earthquakes (Schnellmann *et al.*, 2002; Schwarz-Zanetti *et al.*, 2003).

The failure scars of the described slides are all located on distally steepening slopes (Figs 3B, 8A and 11). Such areas are critical because the gravitational shear stress increases and the shear strength (friction) decreases downwards (Lee & Edwards, 1986; Hampton *et al.*, 1996). The steepest part of the slope, not the average inclination, is critical for slide initiation. Once a slide is initiated, it will destabilize or erode flatter, initially stable zones, as seen in the Weggis Slide and Zinnen Slide examples. In the studied area, slopes with a maximum inclination of <10° generally remained stable during the 1601 AD, magnitude ≈6·2 earthquake. Stronger earthquakes will, however, destabilize flatter slopes (Urgeles *et al.*, 2002), and delta environments will show a different stability from the lateral slopes of a basin because deltaic sedimentation rates are higher and the sediment is coarser and, therefore, more susceptible to liquefaction (Tsuchida & Hayashi, 1971). Additionally, shear strength and, thus, slope stability may also have changed over time, in particular from the Late Glacial to Holocene periods.

A new, ≈2 m thick sediment drape has been deposited on the slide plane of the St Niklausen Slide since its last failure dated at 2420 cal yr BP (Fig. 11). The new drape was not destabilized by the 1601 AD earthquake, indicating either a higher magnitude for the prehistoric earthquake event or a greater stability of the thin recent drape compared with the presumably thicker drape triggered by the 2420 cal yr BP event. This can be explained by the additional weight of a thicker drape, which increases the gravitational stress acting on a potential failure surface.

Massflow

In the examples presented, the massflow deposits form lobes with a radial decrease in thickness and distinct pinch-out points (e.g. Figs 5 and 6). The sharp slope breaks are regarded as responsible for the relatively thick marginal wedges because the sudden break in slope would lead to rapid flow-deceleration, and, as a consequence, to enhanced sediment deposition (Nemec, 1990). The fact that the turbidites generally overlie the massflow deposits indicates relatively high velocities of

the slides and massflows with durations of less than a minute to a few minutes from slide initiation to massflow deposition.

The slope-adjacent, basin-plain sediment is often deformed by the impact and weight of the descending material (e.g. Figs 8C and 12A). As a chaotic-to-transparent seismic facies is a possible acoustic signature for both massflow deposits and deformed basin-plain sediments, the two types of deposits may be indistinguishable on seismic sections. Distinguishing between them is not any easier in cores because the sliding material, as well as the deformed basin-plain sediment, is mainly of Holocene age, and small coherent blocks of these strata can be found in both massflow deposits and deformed basin-plain sediment.

In distal positions, the massflow deposits consist of both relatively small blocks of folded and remoulded strata and a more disintegrated mudclast conglomerate (Fig. 9). These deposits overlie almost undisturbed basin-plain sediment (Figs 5, 6, 8B and 12). The lack of erosion may be explained by hydroplaning, which has been shown to considerably decrease the remobilization capacity of subaqueous massflows (Mosher *et al.*, 1994; Mohrig *et al.*, 1998).

Mass movement-related turbidity current

Two of the four slide complexes described (Weggis and St Niklausen slides) include megaturbidites. These bodies are unusual for the study area with thicknesses clearly exceeding the flood-generated turbidites in these basins. The megaturbidites build clear entities with distinct and relatively smooth upper and lower boundaries that can easily be detected in cores as well as in seismic sections (Figs 8, 9, 12 and 13). Whereas the main, homogeneous, clayey part of the megaturbidite deposits is imaged as a transparent seismic facies, its sandy to silty base results in a strong basal reflection on seismic sections. The graded base and the lack of clasts of older strata within the deposits point towards a complete suspension of the sediment before deposition.

The megaturbidite deposits are thickest in the deepest part of confined basins and overlie either related massflow deposits or undisturbed basin-plain sediment (Figs 7 and 10). In contrast to the open ocean, the suspended material can be easily trapped in the confined basins on fjord and lake floors, resulting in relatively thick turbiditic deposits. Part of the material is likely to have become suspended during sliding, in particular as an effect of the hydraulic changes associated with the sharp lower slope break (Komar, 1971; Kelts & Hsü, 1980; Nemec, 1990). However, only massflows with a certain size and a considerable vertical transport distance will produce substantial turbulence to produce thick megaturbidite deposits. This may explain why no evidence of a (mega)turbidite related to the Chrüztrichter Slide could be detected on seismic sections in the small pond adjacent to the depositional lobe.

Extension (1·5 km^2) and volume (>1 Mio. m^3) of the megaturbidite related to the St Niklausen Slide are rather large compared with the moderate size of the failed slope (0·25 km^2). In fact, the same megaturbidite also overlies five other massflow deposits, which all relate to the same seismic triggering event (2420 cal yr BP; Schnellmann *et al.*, 2002). All these massflows are likely to have produced suspension clouds, which finally merged in the basin plain. Historic descriptions and numerical modelling indicate tsunami and seiche action induced by the multiple slide events of 1601 AD and 2420 cal yr BP (Cysat, 1969; Schnellmann *et al.*, 2002; Schwarz-Zanetti *et al.*, 2003). Siegenthaler *et al.* (1987) calculated that the currents induced by the 1601 AD seiche could have put considerable amounts of sediment into suspension. Consequently, the megaturbidites are interpreted as combined products of sediment put into suspension by multiple sliding, tsunami and seiche action.

Deformation of basin-plain sediment

The deep and relatively far-reaching deformation structures in the slope-adjacent basin-plain sediments underlying the massflow deposits are a striking characteristic common to all four described slide complexes from Lake Lucerne. Although such deep-reaching deformation in overridden lake- and seafloor sediments has been described by other authors (Shilts & Clague, 1992; Syvitski & Schafer, 1996), both the architecture and formation of these deformation structures remain poorly understood.

The seismic expression of the deformed basin-plain sediment can be assigned to two end-members: (1) acoustically layered, coherent blocks that are separated by faults (e.g. Fig. 5); and (2) an unstructured, chaotic-to-transparent seismic facies (e.g. Fig. 12A). The block size tends to be largest at the distal deformation front and decreases towards the proximal part of the deformed zone (Fig. 5A). Where, as a result of deformation and remoulding, the size of internally coherent

and undisturbed blocks falls below the seismic resolution, the acoustic facies turns into a chaotic-to-transparent type. Considering the limited horizontal resolution of the seismic signal (R_{fres} = 6·5 m for 100 m water depth) and the shotpoint spacing of 0·7–0·9 m, a block must have a diameter of several metres to be resolved on a seismic image. A chaotic-to-transparent seismic facies therefore, does not necessarily reflect completely distorted sediment, but can also image deposits including fairly large, internally undisturbed sediment blocks. In fact, the cores taken through acoustically chaotic-to-transparent deposits still revealed undisturbed and coherent sediment packages separated by localized shear zones (Fig. 12B). As such shear zones are sometimes narrow, cores taken through seismically chaotic-to-transparent zones can appear to be undisturbed. Correlation between closely spaced cores is very useful to identify allochthonous sediment blocks and to distinguish disturbed from stratigraphically undisturbed sediment. Where reference cores through undisturbed sediments are missing, or where correlation between individual cores is unclear because of the lack of distinct lamination, palaeomagnetic methods can be applied. Block rotations, folds and shear zones result in unusual changes of the magnetic inclination/declination along core (Schnellmann, 2004).

The quasi-3D seismic information on the general structure and kinematics of deformed basin-plain sediment reveal a range of thin-skinned deformation structures, in particular ramp anticlines and imbricated thrusts (Figs 5, 8C and 12A). The décollement of these structures lies in Late Glacial deposits, except for the St Niklausen Slide, where it is located in mid-Holocene sediments. Seismic lines indicate that the décollements occur in a zone rather than along a single layer (e.g. Fig. 8C). The core through the slope-adjacent basin-plain sediments deformed by the St Niklausen Slide (core 4WS00-3P in Fig. 12B) shows a 1 m thick, intensely deformed basal décollement zone. Above this basal zone, the deformation is less intense and concentrated on small cm- to dm-scale shear zones. Similar to the glide plane of a slide, the depth of such décollements is controlled by the geotechnical properties of the sediment. Although shear strength generally increases with depth, this increase is irregular and weaker layers or zones with a higher pore pressure may control the development of décollements.

In the case of the Zinnen and Weggis slides, parts of the massflow deposits clearly bulge upward as a result of the frontal thrust (Figs 6 and 8). A slight bulge in the lake floor directly above the deformation front can also be seen in the other examples (Figs 5 and 12A). These observations point towards deformation during and possibly after massflow deposition. In the case of the Weggis Slide, it can clearly be shown that the major part of the deformation must have developed syndepositionally.

The typically curved thrust fronts (Figs 2, 7 and 10) indicate a radial compressive stress field and are interpreted as a result of gravity spreading induced by the successive loading of the slope-adjacent basin-plain sediment during deposition of a single massflow. The loading is regarded as an effect of (1) the increasing weight of the massflow wedge and (2) the impact and passage of the descending mass over the sharp lower slope break (Sassa *et al.*, 1985; Lee *et al.*, 1999). A distinct lower slope break is, therefore, regarded as a key element for effective basin-plain deformation because it favours both a sharp deflection of the pathway and the build up of a steep marginal massflow wedge.

Figure 14 shows a schematic model proposed for the development of slope-adjacent basin-plain deformation as a consequence of static and dynamic loading of the lake floor during an individual slide event. It is mainly based on observations from the Zinnen, St Niklausen and Weggis slides, which are on three different scales and, in a simplified way, represent three successive stages in the evolution of basin-plain deformation. As the descending masses reach the basin plain, a marginal wedge begins to build up (Fig. 14A). This wedge grows until it becomes unstable. Its incipient collapse induces gravity spreading (e.g. Schack Pederson, 1987; Schultz-Ela, 2001) and the first overthrusting in the adjacent basin-plain sediment (Fig. 14B). The Zinnen Slide is an example of such an early stage of wedge collapse and the associated deformation of the underlying basin-plain sediment. If the transported volume is high and more slide and massflow material is deposited at the foot of the slope, the depositional wedge grows and, as a consequence, the deformation intensifies and propagates towards more distal areas, leading successively to the geometries displayed by the St Niklausen and Weggis slides (Fig. 14C–E).

CONCLUSIONS

With a dense grid of high-resolution seismic profiles, four slide complexes of variable size

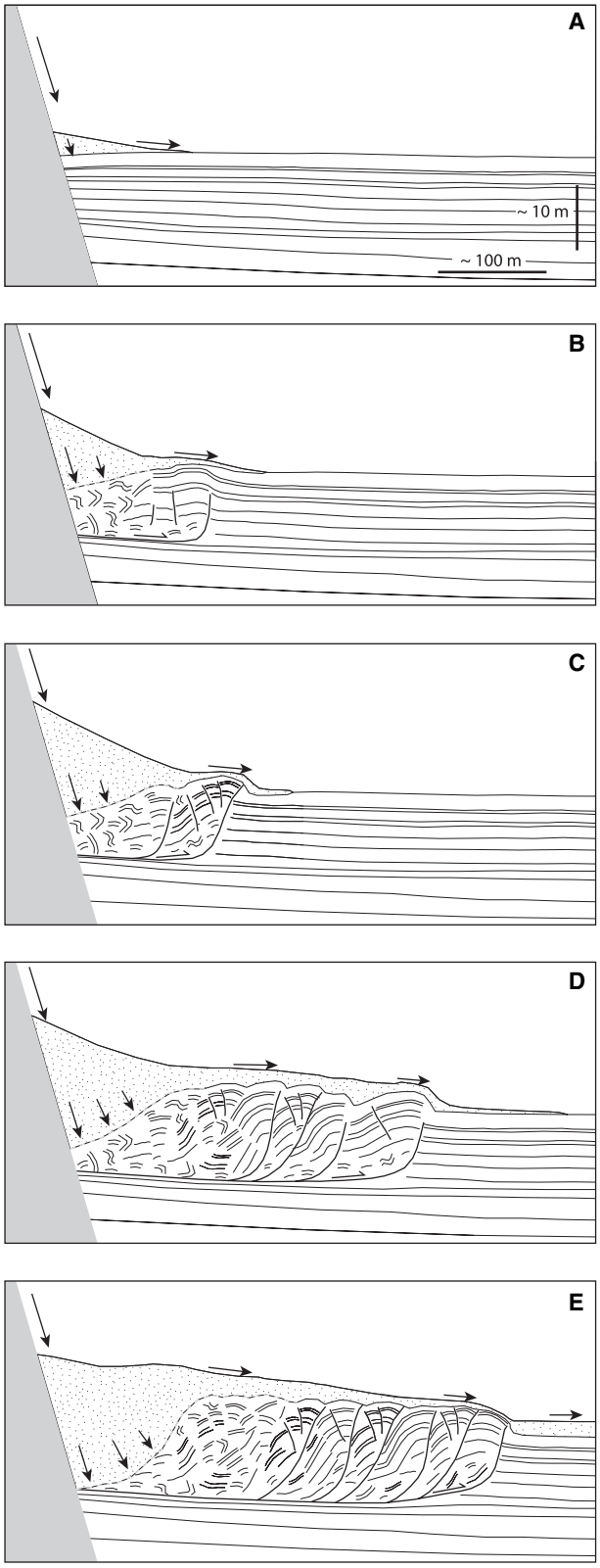

Fig. 14. Schematic kinematic model proposed for the evolution of basin-plain deformation as deduced from the slides studied in Lake Lucerne. Dotted surfaces represent massflow deposits. Loading of the marginal basin floor during a massflow event is regarded as the driving mechanism for the development of basinward propagating fold-and-thrust deformation. Note that, in the very slope-prone area, the boundary (dashed line) between massflow deposits and deformed basin-plain sediments can generally not be identified on seismic sections as a result of their similar chaotic-to-transparent seismic facies.

are shown to have similar architectural characteristics reflecting a common depositional evolution. The distinctive sedimentary and bottom topographic conditions of fjord-type Lake Lucerne have strongly influenced the style of mass movement and the resulting deposits. Thus, the redepositional processes and products analysed in this study are likely to occur in similar settings in both marine and lacustrine environments, as well as those preserved in outcrops.

The following are the principal conclusions of this study:

1. Lateral sliding in Lake Lucerne has induced deep- and far-reaching deformation in the slope-adjacent basin-plain substrate sediments. The deformed zone typically displays a fold-and-thrust belt style structure showing typical analogues to thin-skinned tectonic structures, including ramp anticlines and imbricated thrusts with arcuate strikes and a basal décollement.

2. The mainly syndepositional deformation is interpreted as resulting from increased loading of the basin-plain sediment during deposition of a massflow. The growth of the slope-adjacent massflow wedge leads to a successive propagation of the thrust front towards more distal sediments.

3. The compression and deformation of the flat lake floor is favoured by the peculiar geometry of glacigenic lakes and fjords, which comprises steep slopes with sharp lower slope breaks. This basin geometry, moreover, enables an effective disintegration of the slide slabs and a rapid transformation to massflows and turbidity currents.

4. The scars of the slides typically lie in areas with convex-up curvatures, reflecting the importance of the inclination on the stability of a slope. In the study area, no lateral slides were triggered on slopes with inclinations of <10° by the 1601 AD earthquake. The largely Holocene sedimentary drape on the steep subaqueous slopes of the lake is particularly susceptible to sliding. Thick drapes seem to be less stable compared with thin drapes. This can be explained by the increased gravitational stress induced by the additional weight of a thicker pile of sediments.

5. The massflow deposits build up wedge-shaped depositional geometries with distinct distal terminations. Whereas in seismic sections the deposits show a chaotic-to-transparent facies, clasts of intact strata are abundant in cores.

6. Large massflow deposits are often linked to thick homogenous clay units with a sandy to silty base. Such megaturbidites are focused in the deepest part of confined basins and generally post-date massflow deposition. They are interpreted as the combined products of suspension clouds set up by synchronous sliding and the related tsunami and seiche waves.

ACKNOWLEDGEMENTS

We thank Robert Hofmann for technical assistance and help during fieldwork. Urs Gerber is acknowledged for preparing the coring photographs presented in this paper. Many thanks to Philip Allen, Bas den Brok, Jean-Pierre Burg, Emmanuel Chapron, Alex Densmore, Gregor Eberli, Stéphanie Girardclos, Katrin Monecke and Michael Strasser for discussions of the geological data. Thanks to the reviewers Marc de Batist and Robert W. Duck and to the editor Peter Haughton for the many valuable comments and suggestions. The work was supported by the project PALEOSEIS (Swiss National Science Foundation and Swiss Commission for the Safety of Nuclear Installations).

REFERENCES

Beck, C., Van Rensbergen, P., De Batist, M., Berthier, F., Lallier, S. and **Manalt, F.** (2001) The Late Quaternary infill of Lake Annecy (northwestern Alps): an overview from two seismic-reflection surveys. *J. Paleolimnol.*, **25,** 149–161.

Bouma, A.H. (1987) Megaturbidite; an acceptable term? *Geo-Mar. Lett.*, **7,** 63–67.

Carlson, P.R. and **Karl, H.A.** (1988) Development of large submarine canyons in the Bering Sea, indicated by morphologic, seismic, and sedimentologic characteristics. *Geol. Soc. Am. Bull.*, **100,** 1594–1615.

Chapron, E., Van Rensbergen, P., Beck, C., De Batist, M. and **Paillet, A.** (1996) Lacustrine sedimentary records of brutal events in Lake Le Bourget (northwestern Alps-southern Jura). *Quaternaire*, **7,** 155–168.

Chapron, E., Beck, C., Pourchet, M. and **Deconinck, J.F.** (1999) 1822 earthquake-triggered homogenite in Lake Le Bourget (NW Alps). *Terra Nova*, **11,** 86–92.

Cysat, R. (1969) Collectanea Chronica und denkwürdige Sachen pro Chronica Lucernensi et Helvetiae. [Written 1601]. In: *Quellen und Forschungen zur Kulturgeschichte von Luzern und der Innerschweiz*, Vol. 1 (Ed. J. Schmid), pp. 882–888. Diebold Schilling Verlag, Luzern.

Eyles, N., Boyce, J.I., Halfman, J.D. and **Koseoglu, B.** (2000) Seismic stratigraphy of Waterton Lake, a sediment-starved glaciated basin in the Rocky Mountains of Alberta, Canada and Montana, USA. *Sed. Geol.*, **130,** 283–311.

Fäh, D., Giardini, D., Bay, F., Bernardi, F., Braunmiller, J., Deichmann, N., Furrer, M., Gantner, L., Gisler, M., Isenegger, D., Jimenez, M.J., Kaestli, P., Koglin, R., Masciadri, V., Rutz, M., Scheidegger, C., Schibler, R., Schuerlemmer, D., Schwarz-Zanetti, G., Steimen, S., Sellami, S., Wiemer, S. and **Woessner, J.** (2003) Earthquake catalog of Switzerland (ECOS) and the related macroseismic database. *Eclogae Geol. Helv.*, **96,** 219–236.

Finckh, P., Kelts, K. and **Lambert, A.** (1984) Seismic stratigraphy and bedrock forms in perialpine lakes. *Geol. Soc. Am. Bull.*, **95,** 1118–1128.

Gee, M.J.R., Masson, D.G., Watts, A.B. and **Mitchell, N.C.** (2001) Passage of debris flows and turbidity currents through a topographic constriction: seafloor erosion and deflection of flow pathways. *Sedimentology*, **48,** 1389–1409.

Giovanoli, F., Kelts, K., Finckh, P. and **Hsü, K.J.** (1984) Geological framework, site survey and seismic stratigraphy. In: *Quaternary Geology of Lake Zurich: An Interdisciplinary Investigation by Deep Lake Drilling* (Eds K.J. Hsü and K. Kelts). *Contr. Sedimentol.*, **13,** 5–20.

Hampton, M.A., Lee, H.J. and **Locat, J.** (1996) Submarine landslides. *Rev. Geophys.*, **34,** 33–59.

Hsü, K.J. and **Kelts, K.** (1985) Swiss lakes as a geological laboratory. *Naturwissenschaften*, **72,** 315–321.

Imbo, Y., De Batist, M., Canals, M., Prieto, M.J. and **Baraza, J.** (2003) The Gebra Slide: a submarine slide on the Trinity Peninsula Margin, Antarctica. *Mar. Geol.*, **193,** 235–252.

Kastens, K.A. and **Cita, M.B.** (1981) Tsunami-induced sediment transport in the abyssal Mediterranean Sea. *Geol. Soc. Am. Bull.*, **92,** 845–857.

Kelts, K. (1978) *Geological and sedimentary evolution of Lakes Zurich and Zug.* PhD thesis, ETH Zürich, Zürich, 250 pp.

Kelts, K. and **Hsü, K.J.** (1980) Resedimented facies of 1875 Horgen slumps in Lake Zurich and a process model of longitudinal transport of turbidity currents. *Eclogae Geol. Helv.*, **74,** 271–281.

Kelts, K., Briegel, U., Ghilardi, K. and **Hsü, K.J.** (1986) The limnogeology-ETH coring system. *Schweiz. Z. Hydrol.*, **48,** 104–115.

Kenyon, N.H. (1987) Mass-wasting features on the continental-slope of Northwest Europe. *Mar. Geol.*, **74,** 57–77.

Komar, P.D. (1971) Hydraulic jumps in turbidity currents. *Geol. Soc. Am. Bull.*, **82,** 1477–1487.

Lee, H.J. and **Edwards, B.D.** (1986) Regional method to assess offshore slope stability. *J. Geotech. Eng.*, **112,** 489–509.

Lee, S.H., Chough, S.K., Back, G.G., Kim, Y.B. and **Sung, B.S.** (1999) Gradual downslope change in high-resolution acoustic characters and geometry of large-scale submarine debris lobes in Ulleung Basin, East Sea (Sea of Japan), Korea. *Geo-Mar. Lett.*, **19,** 254–261.

Lemcke, G. (1992) *Ablagerungen aus Extremereignissen als Zeitmarken der Sedimnentationsgeschichte im Becken von Vitznau/Weggis (Vierwaldstättersee, Schweiz).* MS thesis, Institut für Geologie und Dynamik der Lithosphäre der Georg-August-Universität Göttingen, Göttingen, 154 pp.

Locat, J. and **Lee, H.J.** (2000) Submarine landslides: advances and challenges. *Proceedings of the 8th International Symposium on Landslides*, Cardiff, UK, June 2000, 30 pp.

Mohrig, D., Whipple, K.X., Hondzo, M., Ellis, C. and **Parker, G.** (1998) Hydroplaning of subaqueous debris flows. *Geol. Soc. Am. Bull.*, **110,** 387–394.

Mosher, D.C., Moran, K. and **Hiscott, R.N.** (1994) Late Quaternary sediment, sediment mass-flow processes and slope stability on the Scotian Slope, Canada. *Sedimentology*, **41,** 1039–1061.

Mulder, T. and **Cochonat, P.** (1996) Classification of offshore mass movements. *J. Sed. Res.*, **66,** 43–57.

Mullins, H.T., Eyles, N. and **Hinchey, E.J.** (1991) High-resolution seismic stratigraphy of Lake McDonald, Glacier-National-Park, Montana, USA. *Arct. Alpine Res.*, **23,** 311–319.

Nakajima, T. and **Kanai, Y.** (2000) Sedimentary features of seismoturbidites triggered by the 1983 and older historical earthquakes in the eastern margin of the Japan Sea. *Sed. Geol.*, **135,** 1–19.

Nardin, T.R., Hein, F.J., Gorsline, D.S. and **Edwards, B.D.** (1979) A review of mass movement processes, sediment and acoustic characteristics, and contrasts in slope and base-of-slope systems versus canyon-fan-basin floor systems. In: *Geology of Continental Slopes* (Eds L.J. Doyle and O.H. Pilkey). *Int. Assoc. Sedimentol. Spec. Publ.*, **27,** 61–73.

Nemec, W. (1990) Aspects of sediment movement on steep delta slopes. In: *Coarse-grained Deltas* (Eds A. Colella and D.B. Prior). *Int. Assoc. Sedimentol. Spec. Publ.*, **10,** 29–73.

Piper, D.J.W., Cochonat, P. and **Morrison, M.L.** (1999) The sequence of events around the epicentre of the 1929 Grand Banks earthquake: initiation of debris flows and turbidity current inferred from sidescan sonar. *Sedimentology*, **46,** 79–97.

Prior, D.B. and **Coleman, J.M.** (1978) Disintegrating retrogressive landslides on very-low-angle subaqueous slopes, Mississippi Delta. *Mar. Geotech.*, **3,** 37–60.

Prior, D.B., Wiseman, W.J. and **Gilbert, R.** (1981) Submarine slope processes on a fan delta, Howe Sound, British Columbia. *Geo-Mar. Lett.*, **1,** 85–90.

Prior, D.B., Bornhold, B.D. and **Johns, M.W.** (1984) Depositional characteristics of a submarine debris flow. *J. Geol.*, **92,** 707–727.

Sassa, K., Kaibori, M. and **Kitera, N.** (1985) Liquefaction and undrained shear of torrent deposits as the cause of debris flows. In: *Proceedings of the International Symposium on Erosion, Debris Flow and Disaster Prevention* (Ed. A. Takei), Tsukuba, Japan, pp. 231–236.

Schack Pederson, S.A. (1987) Comparative studies of gravity tectonics in Quaternary sediments and sedimentary rocks related to fold belts. In: *Deformation of Sediments and Sedimentary Rocks* (Eds M.E. Jones and R.M.F. Preston). *Geol. Soc. Spec. Publ.*, **29,** 165–179.

Schnellmann, M. (2004) *Late quaternary mass movements in a perialpine lake (Lake Lucerne, Switzerland) – sedimentary processes, natural hazards and paleoseismic reconstructions*. PhD thesis, ETH Zürich, Zürich, 132 pp.

Schnellmann, M., Anselmetti, F.S., Giardini, D., McKenzie, J.A. and **Ward, S.N.** (2002) Prehistoric earthquake history revealed by lacustrine slump deposits. *Geology*, **30,** 1131–1134.

Schultz-Ela, D.D. (2001) Excursus on gravity gliding and gravity spreading. *J. Struct. Geol.*, **23,** 725–731.

Schwarz-Zanetti, G., Deichmann, N., Fäh, D., Giardini, D., Jimenez, M.J., Masciadri, V., Schibler, R. and **Schnellmann, M.** (2003) The earthquake in Unterwalden on September 18, 1601 – a historico-critical macroseismic evaluation. *Eclogae Geol. Helv.*, **96,** 441–450.

Shilts, W.W. and **Clague, J.J.** (1992) Documentation of earthquake-induced disturbance of lake sediments using subbottom acoustic profiling. *Can. J. Earth Sci.*, **29,** 1018–1042.

Siegenthaler, C., Finger, W., Kelts, K. and **Wang, S.** (1987) Earthquake and seiche deposits in Lake Lucerne, Switzerland. *Eclogae Geol. Helv.*, **80,** 241–260.

Sturm, M. and **Matter, A.** (1978) Turbidites and varves in Lake Brienz (Switzerland); deposition of clastic detritus by density currents. In: *Modern and Ancient Lake Sediments* (Eds A. Matter and M.E. Tucker). *Int. Assoc. Sedimentol. Spec. Publ.*, **2,** 147–168.

Syvitski, J.P.M. and **Schafer, C.T.** (1996) Evidence for an earthquake-triggered basin collapse in Saguenay Fjord, Canada. *Sed. Geol.*, **104,** 127–153.

Terzaghi, K. (1956) Variety of submarine mass failures. *Proceeding of the 8th Texas Conference on Soil Mechanics and Foundation Engineering*, 41 pp.

Tsuchida, H. and **Hayashi, S.** (1971) Estimation of liquefaction potential of sandy soils. In: *Proceedings of the Third Joint Meeting U.S. Japan Panel on Wind and Seismic Effects UJNR*, Tokyo, pp. 91–109.

Urgeles, R., Locat, J., Lee, H.J. and **Martin, F.** (2002) The Saguenay Fjord, Quebec, Canada: integrating marine geotechnical and geophysical data for spatial seismic slope stability and hazard assessment. *Mar. Geol.*, **185,** 319–340.

Van Rensbergen, P., De Batist, M., Beck, C. and **Chapron, E.** (1999) High-resolution seismic stratigraphy of glacial to interglacial fill of a deep glacigenic lake: Lake Le Bourget, Northwestern Alps, France. *Sed. Geol.*, **128,** 99–129.

Manuscript received 4 November 2003;
revision accepted 4 November 2004